2010 IEEE-RAS International Conference on Humanoid Robots
Nashville, TN, USA, December 6-8, 2010

Development of a Biped Robot with Torque Controlled Joints

Christian Ott, Christoph Baumgärtner, Johannes Mayr, Matthias Fuchs, Robert Burger,
Dongheui Lee, Oliver Eiberger, Alin Albu-Schäffer, Markus Grebenstein, and Gerd Hirzinger

Abstract— **This paper gives an overview of the development of a novel biped walking machine. The robot is designed as an experimental system for studying biped locomotion based on torque controlled joints. As an underlying drive technology, the torque controlled joint units of the DLR-KUKA-Lightweight-Robot are employed. The relevant design choices for using this technology in a biped robot with integrated joint torque sensors are highlighted and some first experimental results using a conventional ZMP based control scheme are discussed.**

I. INTRODUCTION

Besides two-handed dexterous manipulation, perception, and higher level-reasoning, biped locomotion traditionally is one of the major research fields in humanoid robots. While locomotion with wheels allows for a relatively firm support, wheeled systems have clear limitations in domestic environments due to a larger support area and their incapacity to overcome small obstacles or climbing of stairs. Since human environments are highly adapted to the human body shape, it is natural to consider human-like biped locomotion as an alternative to wheel-based systems for domestic service robotics scenarios.

These application oriented benefits of legged locomotion come at a certain cost from a control point of view. In particular, one has to cope with changing contact conditions in single support and double support phases. Moreover, the reduced support area, which allows for motion of the robot in narrow spaces, presents an additional difficulty for plain balancing as well as for locomotion. Biped locomotion, thus, offers several new challenges to the control engineer.

In the robotics community, several different approaches for tackling the problem of biped walking have been proposed. The following overview will focus on the hardware aspects rather than on control issues. It is widely recognized that the first biped robots have been developed in Prof. Kato's lab at the University of Waseda. This line of research still influences the biped robot literature and recently lead to the development of WABIAN-II [1], the first fully actuated robot which achieved walking with stretched knees. One of the major breakthroughs was the introduction of the zero moment point (ZMP) by Vukobratovic [2]. The concept of the ZMP was utilized in the design and control of several impressive biped robots [3], [4], [5], [6].

The humanoid robot HRP-3 [7], developed at AIST, allows for use in dusty and rainy environments due to specialized mountings. It is also equipped with multifingered hands for manipulation. HRP-3 is a further development of HRP-2[4], [8] a humanoid robot which nowadays is used for research in many labs. The latest development in the HRP series is HRP-4, a slim walking machine with female shape [9].

All authors, except D. Lee, are with the Institute of Robotics and Mechatronics, German Aerospace Center (DLR e.V.), D-82234 Wessling, Germany. Corresponding Author: Ch. Ott, email:christian.ott@dlr.de

D. Lee is with the Department of Electrical Engineering and Information Technology, Technical University of Munich, D-80290 Munich, Germany

Fig. 1. DLR-Biped: A biped walking machine with torque controlled joints.

The integration of vision for real-time step planning was achieved in H6 and H7 [10], [11], humanoid robots developed at the University of Tokyo, and Johnnie [12] and its successor Lola [13] from the Technical University of Munich. Apart from academic research, the developments on biped walking were also largely influenced by company developments like Honda's Asimo [14], Sony's small scale humanoid robot [15], and Toyota's partner robots [16].

The above-mentioned robots can be regarded as belonging to a class of electrically driven fully actuated walking machines, which are mainly designed as rigid-body systems in which only a small fraction of compliant material deliberately was introduced at strategic locations in the foot for handling the ground impacts during walking.

The humanoid robot CB [17], built by Sarcos, uses hydraulic actuation and allows for joint torque sensing. In [18], joint torque sensing based compliance control was used for biped balancing. It was shown that this control approach can lead to very robust behavior in balancing. These results on biped balancing confirm the robustness properties found in similar controllers developed for manipulation tasks using robot manipulators [19], [20], [21] and a humanoid upper body system [22], [23].

Series elastic actuators [24] employ a compliant element in the drive train in order to support sensitive joint torque control. These type of actuators have successfully been applied to bipedal walking in 2D [25] and 3D [26]. While

compliance in the actuation is beneficial for handling high-frequency impacts and for implementing force control, it requires additional vibration damping control for positioning tasks.

Passive dynamic walkers, pioneered by the works of McGeer [27], present a fundamentally different type of walking machines. In these machines simple mechanical principles are exploited for designing a mechanism which allows for a stable limit cycle. While these systems originally have been purely passive mechanisms, these concepts are nowadays used in dynamic limit cycle walking machines, in which actuators are integrated for allowing to influence the limit cycle and extend the previous purely passive systems to a larger range of environments and motion patterns (see e.g. [28], [29], [30]). While these systems often show advantages in terms of power consumption and result in naturally looking gaits (due to straight leg walking), their application areas still are relatively limited compared to fully actuated biped robots.

In the present paper, the development of an electromechanically actuated biped robot with integrated joint torque sensors is presented (see Fig.1). The robot design aims at a system, which allows the implementation of position based walking control laws as well as compliant joint torque control for studying the use of joint torque sensing and impedance control in biped walking. Joint torque sensing and control has been successfully integrated in the technology of the DLR-KUKA-Lightweight-Robot (LWR) [31]. In [19], [20] the advantages of joint torque control for manipulation were shown based on a robot model, which explicitly considered the robot's elasticity in the joints. From our previous experience on manipulation tasks, we believe that similar control approaches can also be useful for the balancing and walking problems arising in biped robots. In this paper the design considerations are discussed, which led to the development of an experimental biped robot based on the joint technology of the LWR in a development time of less than 10 months.

II. Mechanical Design

A. Specification

The development goal was to build a biped robot with integrated joint torque sensors as an experimental platform for studying different approaches for biped balancing and walking. In order to keep the development time and cost low, it was decided to use the well-proven joint technology of the LWR as a basis. The robot should be stiff enough for allowing to implement classical ZMP based walking controllers.

As general design guidelines, the biped robot should, on the one hand, be designed such that it is strong enough for performing a squat motion on one leg, which is considered as a benchmark for tasks like climbing stairs. Furthermore, it should be capable of the torque and velocity requirements for dynamic walking[1].

B. The DLR-KUKA-Lightweight-Robot

The 7 degrees-of-freedom (DOF) LWR [31], which is commercially available from KUKA Roboter GmbH, is a kinematically redundant manipulator arm, which was designed with the aim to achieve a high load-to-weight ratio (about 1:1). This led to the use of small customized motors (available from RoboDrive GmbH) and high gear ratios. In order to handle the elasticity of the gears and to allow for sensitive force and impedance control as required for dexterous manipulation, the close integration of joint torque sensors at the power output side of the drive units was one of the main design issues. Moreover, except for the external power supply, all required power converters and digital electronics are integrated into the robots structure. Figure 2 shows the robot arm and the key parameters of the different drive units.

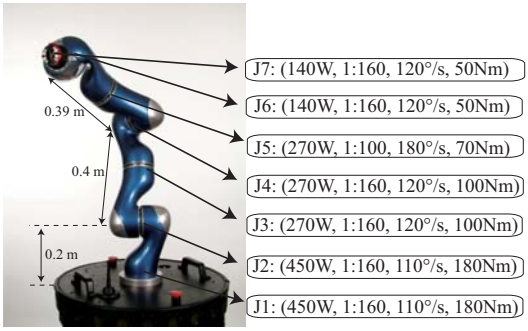

Fig. 2. The DLR-Lightweight-Robot-III. For each joint, the nominal motor power, the gear transmission, the maximal joint velocity and the maximal joint torque are given.

C. Kinematics

In order to keep the overall weight low, the leg kinematics was restricted to a kinematically non-redundant configuration with six DOF. This allows to control the motion of the center of mass (COM), the spatial motion of the swing leg with respect to the stance leg, and the trunk orientation. Similar to most biped robots, an anthropomorphic kinematic configuration with 3 DOF in the hip, one DOF in the knee and 2 DOF in the ankle was chosen. The overall kinematic structure is shown in Fig. 3. For the kinematic structure of the hip and the knee, the link structure of the LWR could be used, while the design of the lower leg and the ankle required a new design. Due to the adoption of the LWR segments in the hip, the length of the upper leg was fixed to 0.4 m.

In order to avoid the kinematic singularity when the joint axes of the first and third joint intersect, a joint offset was introduced to the second joint. The kinematic structure of the pitch joints of the LWR allow a joint angle range of up

[1]The term "dynamic walking" is used in two different contexts in the literature. It refers to either dynamic limit cycle walking, or to dynamic walking as opposed to static walking in the sense that the projection of the center of gravity may leave the support polygon. In the present paper, the term is used in the latter sense.

to 120 degrees from the outstretched configuration. The hip angle α (see Fig. 3) was chosen as 20 degrees in the nominal configuration, with the possibility of manual adjustment by ± 10 degrees, allowing for good mechanical stability and a motion range up to +50 degrees in the second hip axis.

The distance from the knee to the ankle was chosen the same as between hip and knee (i.e. 0.4 m). The two ankle axes are attached to a universal joint, where the fifth axis is placed within the universal joint, responsible for its sideways flexion. The drive unit of the sixth axis is located just below the knee axis in order to locate its mass as high as possible within the lower leg. It actuates the ankle flexion/extension via a rod, which is ranging over the fifth axis (see Fig. 4). When the ankle roll axis is in the zero configuration, the bar kinematics results in a rigid transmission with unit transmission ratio. This special arrangement on the one hand introduces a coupling between the ankle joint axes, on the other hand allows for a slim and powerful ankle, with low inertia. Furthermore, it guarantees that during surface contact between the foot and the ground, the pitch axis stays parallel to the ground. For locomotion along the sagittal axis the pitch axis is mainly responsible for the forward walking, while the roll axis is mainly responsible for the lateral COM shift. During dynamic walking, a large motion of the pitch axis is required compared to the motion of the roll axis. Therefore, the chosen axis configuration with the pitch axis as the terminal joint is beneficial during dynamic walking on flat ground, since it leads to smaller joint motions in the upper leg.

In order to avoid a too close placement of the knee structures during walking motions, the foot distance is chosen smaller than the hip distance. The joint angle limits are shown in Fig. 3. The overall dimensions of the robot are depicted in Fig. 5. Its total weight is about 49.2 kg, with 18 kg in the trunk, 8.2 kg in the upper legs, and 7.1 kg in the lower legs. Below the ankle joint, a 6-DOF force torque sensor is integrated. For the stance, a first approach with a planar, rectangular foot with a foot area of 0.095×0.25 m and a minimal damping layer was implemented. Further development shall be focused on the design of the foot geometry, damping of heel and ball, as well as the introduction of toes for stabilization of dynamic walking.

D. Drive System

In order to meet the requirements of legged locomotion, the joint modules in the LWR were rearranged to match the torque and speed criteria from three different benchmark motions. As benchmark motions, a squat motion up to 90 degrees in the knee joint, a slow squat motion on one leg, and a forward walking motion were chosen. Dynamic simulations using OpenHRP3 and Simpack were used to predict speed and torque requirements at walking speeds of up to 1.35 km/h for the proposed configuration, using LWR modules. The generation of the walking motion will be briefly discussed in Section IV. Figure 7 shows a typical velocity and torque trajectory for the knee and ankle pitch joint in a simulated walking motion with a stride length of $24cm$ and a step time

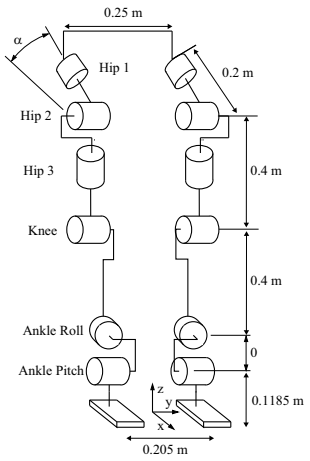

Joint Limits

Joint	min [°]	max [°]
1 - Hip 1	-170	170
2 - Hip 2 (Pitch)	-120	60
3 - Hip 3 (Yaw)	-170	170
4 - Knee	-115	115
5 - Ankle Roll	-20	20
6 - Ankle Pitch	-45	45

Fig. 3. Kinematic structure. The hip angle α can be manually adjusted to 10, 20, and 30 degrees.

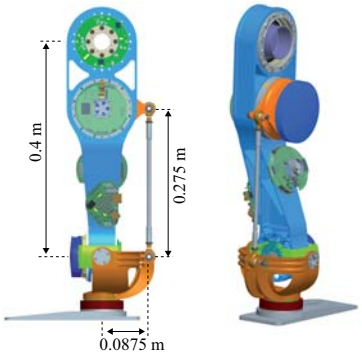

Fig. 4. Design of the ankle kinematics.

of $0.8s$. The composition of motor and gear units in the legs and their respective location in the original robot arm are depicted in Table I.

Figure 6 shows a crossection of the ankle joint, seen from below. The center shows the smaller drive of axis 5, operating the roll motion, which is enclosed by the connecting structure for the pitch joint. In the upper part of the picture the connecting rod between the joint module in the background and the ankle is visible.

III. Measurement & Control System

Except for the force/torque sensors in the feet, the complete control hardware consists of off-the-shelf components.

TABLE I
Joint Drive Specification

Joint	Motor Power $[W]$	Gear Ratio	$\dot{q}_{\max}$ $[^\circ/s]$	$\tau_{\max}$ $[Nm]$	LWR Joint #
Hip 1	270	160	120	100	J3
Hip 2	270	160	120	100	J4
Hip 3	270	100	180	70	J5
Knee	450	160	110	180	J2
Ankle R	140	160	120	50	J6
Ankle P	450	160	110	180	J1

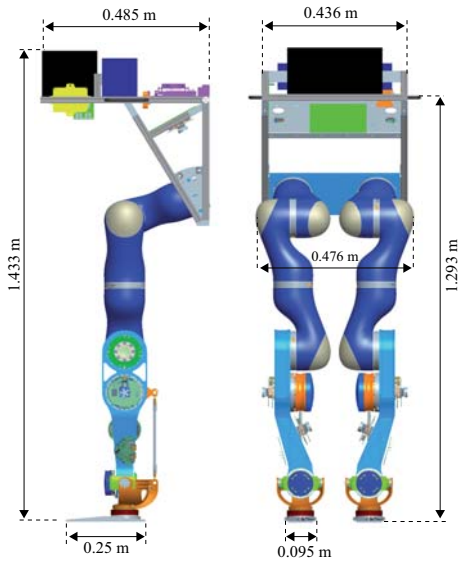

Fig. 5. Size of the DLR-Biped.

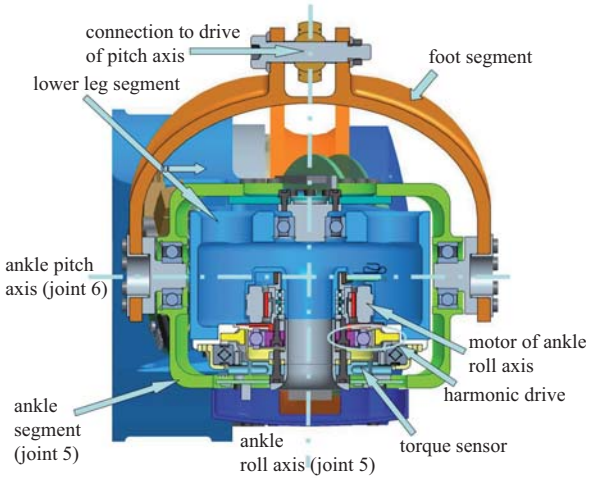

Fig. 6. Assembly in the ankle, seen from the foot. The blue parts correspond to the segments of the lower leg. The parts connected to the foot are shown in orange color.

The power supply consists of a Lithium-Iron-Phosphate accumulator (LiFePO4- or LFP-battery) with a nominal voltage of 48 volts and several DCDC-converter modules to cope with the demanded onboard supply voltages of 48V, 24V, 12V, and 5V. The LFP-battery can handle high discharge and charge currents (for the biped robot 60A/20A) without loss of lifetime. Thus the battery is able to manage high motor current peaks as well as short charging times. The DCDC-converter modules from PULS GmbH transfer the battery voltage into suitable voltage levels for the onboard computer, the emergency stop system, the wireless network adapter, the IMU and the force torque sensors in the feet. With a fully charged battery, the power supply is able to run the biped robot for up to five hours in high duty mode.

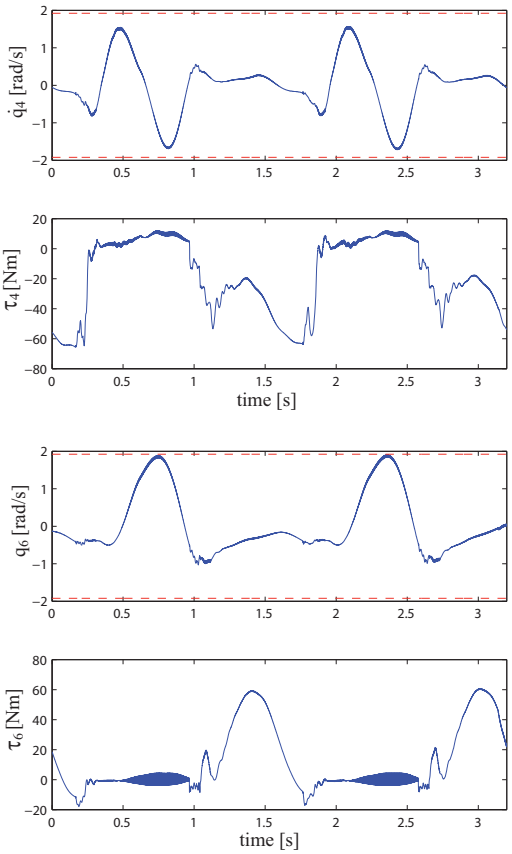

Fig. 7. Velocity and torque for the knee and the ankle pitch axis in a simulated walking motion.

A. Sensors

The joint units of the DLR-KUKA-Lightweight-Arm are equipped with a motor position and a link position sensor, as well as a joint torque sensor from SensoDrive GmbH. In addition to these intrinsic sensors of the drive units, customized six-axis force torque sensors are used in each foot for measuring the contact forces and consequently the ZMP location. The measurement range of the sensors allows forces up to 1000 N and torques up to 80 Nm. As a communication protocol for the force torque sensors, RS485 communication with a sampling rate of 2 ms and a datarate of 230400 Baud is used.

Additionally, an inertia measurement unit (IMU) from XSens Technologies BV is integrated in the trunk. IMU data is read with a sampling time of 4 ms and a datarate of 460800 Baud via standard RS232 communication.

B. Computer system

The DLR-Biped is controlled from an onboard computer in the trunk. We use a 2.8 GHz dual core mobile CPU in a Mini-ITX mainboard. As a realtime operating system, VxWorks is employed. For communication between the drive units and the main computer, the Sercos II bus interface of the DLR-KUKA-Lightweight-Arms is used and implemented by a PCI sercos interface card from Beckhoff. We have integrated two

separate Sercos II rings - one for each leg - which are synchronized by the Beckhoff hardware. The bus is running with a datarate of 8 MBaud, such that all sensor data from the drive units is available in a 1ms cycling time. The force torque sensors are directly connected to the RS485 ports of a PCIe interface card. Figure 8 shows a sketch of the assembly on the trunk of the robot including the IMU, the realtime computer, and the battery.

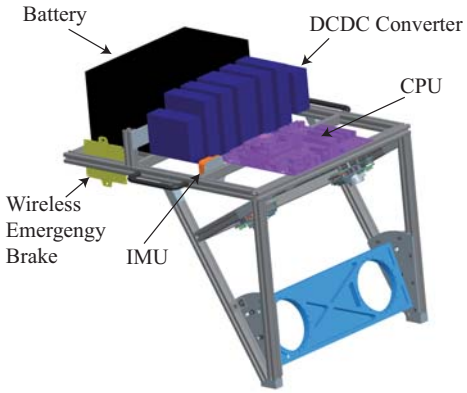

Fig. 8. Assembly in the trunk.

C. Software

The control algorithms have been implemented in Matlab/Simulink and are running on the realtime system using the External Mode of the Matlab Realtime Workshop. The model execution is synchronized to the Sercos II hardware. For network communication with the host PC, a wireless LAN connection is used.

For testing the control algorithms in advance, dynamical simulations of the controlled robot were performed using OpenHRP3 [32] and Simpack. In order to interface the developed controllers within Matlab/Simulink with the physics simulator of OpenHRP3, a shared memory based communication interface has been developed based on the "ard" communication tools [33]. This allows for a flexible hardware in the loop simulation of the complete control architecture.

IV. Experiments

A. Dynamic Walking

As a first experiment, a classical ZMP based approach as shown in Fig. 9 was implemented. Based on a list of predetermined footsteps, a ZMP reference trajectory is generated. From this, the trajectory of the COM is calculated online by using preview control [34]. Due to the use of preview control, a delay is introduced in the generation of the COM motion which has to be taken into account for the trajectories of the swing foot and the torso. Depending on the desired footsteps and the step time, respectively the single support time, the position and orientation of the swing leg and the orientation of the torso are generated by polynomial functions. The COM motion is controlled according to the real ZMP calculated from the six-axis force torque sensors

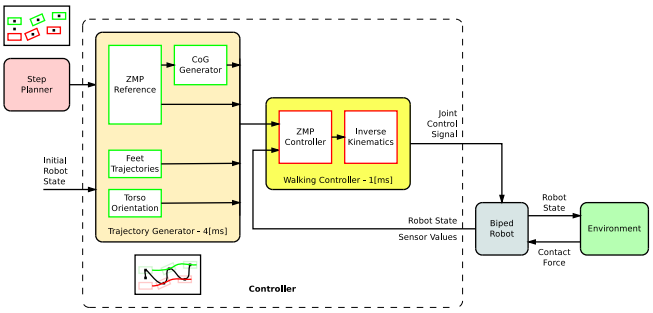

Fig. 9. Walking Control Structure

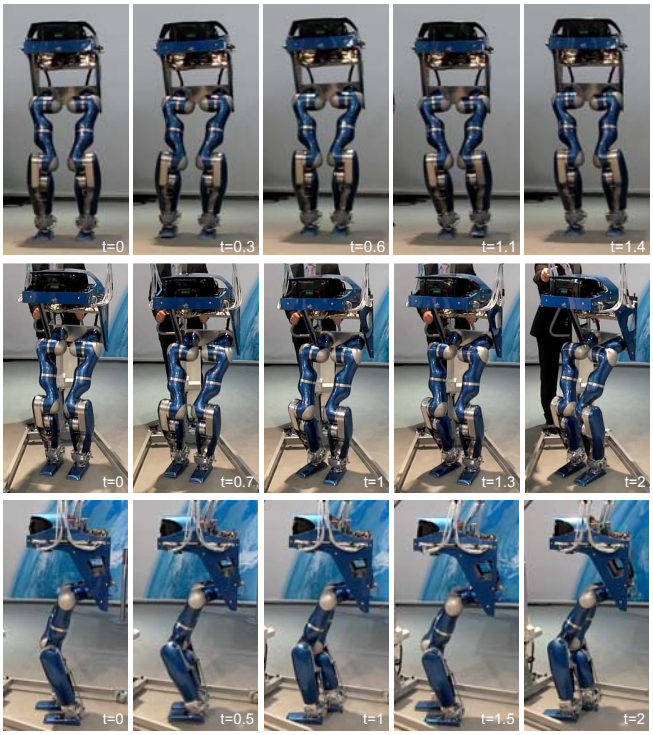

Fig. 10. Snapshots of different walking experiments: Sidewards walking (step length: $0.07[m]$, step time: $0.8[s]$), Turning motion (step time: $0.8[s]$), Forward walking (step length: $0.12[m]$, step time: $0.8[s]$).

[35]. Finally, the joint angles are calculated by using the COM Jacobian with embedded motion [36]. For higher accuracy of the position control, the joint torques caused by gravity are calculated as in [37] and used as an additional feed-forward control input.

For testing the hardware and the walking control algorithm from Fig. 9, multiple motion primitives like walking forward, sidewards, or turning have been successfully tested as well as some more complicated motions generated by a tree-based footstep planner [11]. Some snapshots of the walking experiments are shown in Fig. 10.

Another experiment of straight walking with a stride length of $0.2[m]$, a step height of $0.03[m]$ and a step time of $0.8[s]$ was done to check the velocity and torque limits of the joints. The corresponding joint positions and torques for the right leg are shown in Fig. 11 and 12. In the second and fourth section, the left leg is the stance leg and one

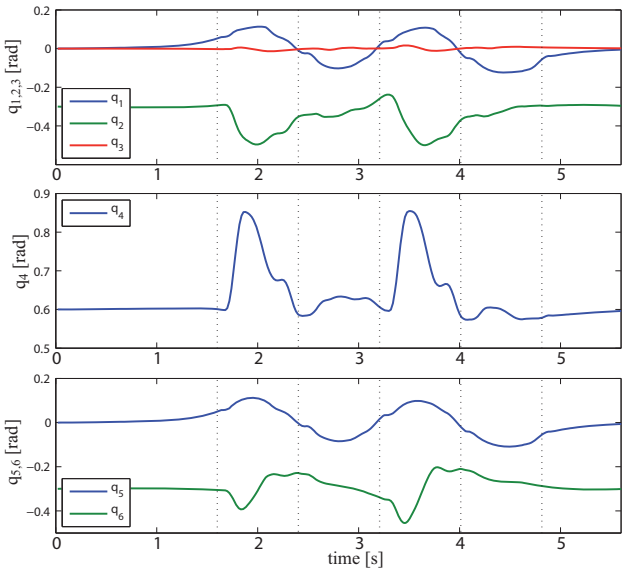

Fig. 11. Joint angles for the right leg during a forward walking motion: (1) hip, (2) knee, (3) ankle.

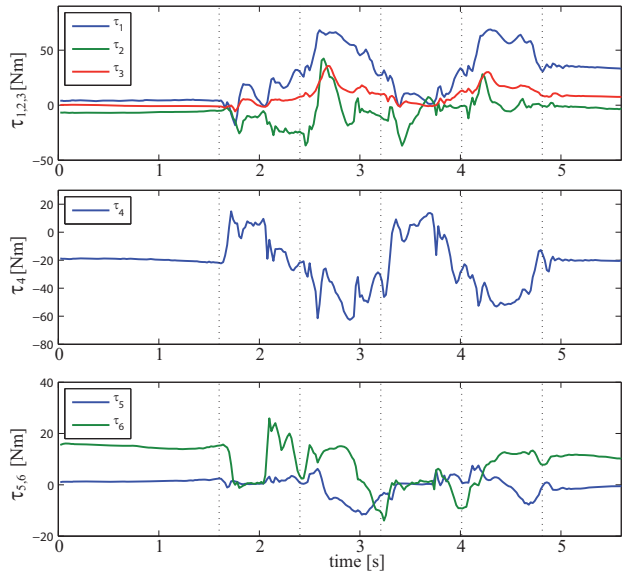

Fig. 12. Joint torque for the right leg during a forward walking motion: (1) hip, (2) knee, (3) ankle

can observe the lifting and a two-staged lowering motion of the right foot in the knee trajectory. The experiments have demonstrated that state-of-the-art ZMP based position controlled methods can be used successfully with the new developed system. It proves to also effectively damp oscillations caused by the elasticity of the gears, the torque sensors and the structure.

B. User Interface

In addition to the demonstration of walking pattern generation with footsteps from a simple step planner in the previous section, commanding different motion primitives from an intuitive user interface was demonstrated. In the latter case, a human user controls the robot's behavior in an online

Fig. 13. Human gesture commands and corresponding robot's gait primitives: (top left) side walk right/left, (top right) go back, (bottom left) come, (bottom right) turn clockwise/counterclockwise.

manner using his/her body gestures based on the algorithm in [38]. For this purpose, human's gesture commands are captured using a motion capture suit from XSens and each gesture command is trained as a continuous hidden Markov model (HMM) by the EM algorithm [39]. After the training procedure, human gesture commands are recognized online by using the HMM forward algorithm, and the recognition result triggers the appropriate walking primitive of the robot. In this experiment, seven gesture commands are trained and recognized: 'idle' state, 'come', 'go back', 'sidewalk right', 'sidewalk left', 'turn clockwise', and 'turn counterclockwise'. Figure 13 illustrates the human's gesture commands and the corresponding robot's gait primitives.

V. SUMMARY AND FUTURE WORKS

In this paper, conceptual design issues related to the construction of a torque controlled biped robot based on the joint technology of the KUKA-DLR-Lightweight-Robots were presented. The system was developed in a period of about 10 month and was first shown to the public during the Automatica fair in June 2010 using an algorithm for dynamic ZMP based walking.

Future work with this system will focus on the roles of torque sensing, joint flexibility, and impedance control in biped walking. From a hardware point of view, in particular a modification of the simple flat foot will be considered.

REFERENCES

[1] Y. Ogura, H. Aikawa, K. Shimomura, H. Kondo, A. Morishima, H. ok Lim, and A. Takanishi, "Development of a new humanoid robot wabian-2," in *IEEE Int. Conf. on Robotics and Automation*, 2006, pp. 76–81.

[2] M. Vukobratovic and Y. Stepanenko, "On the stability of anthropomorphic systems," *Mathematical Biosciences*, vol. 15, pp. 1–37, 1972.

[3] K. Hirai, M. Hirose, Y. Haikawa, and T. Takenaka, "The development of honda humanoid robot," in *IEEE Int. Conf. on Robotics and Automation*, 1998.

[4] K. Kaneko, F. Kanehiro, S. Kajita, H. Hirukawa, T. Kawasaki, M. Hirata, K. Akachi, and T. Isozumi, "Humanoid robot hrp-2," in *IEEE Int. Conf. on Robotics and Automation*, 2004, pp. 1083–1090.

[5] I. Park, J. Kim, J. Lee, and J. Oh, "Mechanical design of the humanoid robot platform, hubo," *Advanced Robotics*, vol. 21, no. 11, 2007.

[6] B. You, Y. Choi, M. Jeong, D. Kim, Y. Oh, C. Kim, J. Cho, M. Park, and S. Oh, "Network-based humanoids mahru and ahra," in *International Conference on Ubiquitious Robots and Ambient Intelligence*, 2005, pp. 376–379.

[7] K. Kaneko, K. Harada, F. Kanehiro, G. Miyamori, and K. Akachi, "Humanoid robot hrp-3," in *IEEE/RSJ Int. Conference on Intelligent Robots and Systems*, 2008, pp. 2471–2478.

[8] N. Kanehira, T. Kawasaki, S. Ohta, T. Isozumi, T. Kawada, F. Kanehiro, and K. Kaneko, "Design and experiments of advanced leg module (hrp-2l) for humanoid robot (hrp-2) development," in *IEEE/RSJ Int. Conference on Intelligent Robots and Systems*, 2002, pp. 2455–2460.

[9] K. Kaneko, F. Kanehiro, M. Morisawa, K. Miura, and S. N. S. Kajita, "Cybernetic human hrp-4c," in *Humanoids*, 2009, pp. 7–14.

[10] K. Nishiwaki, T. Sugihara, S. Kagami, F. Kanehiro, M. Inaba, and H. Inoue, "Design and development of research platform for perception-action integration in humanoid robot: H6," in *IEEE/RSJ Int. Conference on Intelligent Robots and Systems*, 2000, pp. 88–95.

[11] J. Kuffner, S. Kagami, K. Nishiwaki, M. Inaba, and H. Inoue, "Online footstep planning for humanoid robots," in *Proceedings of the IEEE International Conference on Robotics and Automation*, 2003.

[12] M. Gienger, K. Löffler, and F. Pfeiffer, "Design and control of a biped walking and jogging robot," in *2nd International Conference on Climbing and WalkingRobots (CLAWAR)*, 1999.

[13] S. Lohmeier, T. Buschmann, and H. Ulbrich, "System design and control of anthropomorphic walking robot lola," *IEEE/ASME Transactions on Mechatronics*, vol. 14, no. 6, pp. 658–666, 2009.

[14] Y. Sakagami, R. Watanabe, C. Aoyama, S. Matsunaga, N. Higaki, and K. Fujimura, "The intelligent asimo: system overview and integration," in *IEEE/RSJ Int. Conference on Intelligent Robots and Systems*, 2002, pp. 2478–2483.

[15] T. Ishida, Y. Kuroki, and J. Yamaguchi, "Mechanical system of a small biped entertainment robot," in *IEEE/RSJ Int. Conference on Intelligent Robots and Systems*, 2003, pp. 1129–1134.

[16] R. Tajima, D. Honda, and K. Suga, "Fast running experiments involving a humanoid robot," in *IEEE Int. Conf. on Robotics and Automation*, 2009, pp. 1571–1576.

[17] G. Cheng, S.-H. Hyon, J. Morimoto, A. Ude, G. Colvin, W. Scroggin, and S. C. Jacobsen, "Cb: A humanoid research platform for exploring neuroscience," in *HUMANOIDS*, 2006.

[18] S.-H. Hyon and G. Cheng, "Gravity compensation and full-body balancing for humanoid robots," in *IEEE-RAS International Conference on Humanoid Robots*, 2006, pp. 214–221.

[19] C. Ott, A. Albu-Schäffer, A. Kugi, and G. Hirzinger, "On the passivity based impedance control of flexible joint robots," *IEEE Transactions on Robotics*, vol. 24, no. 2, pp. 416–429, 2008.

[20] A. Albu-Schäffer, Ch. Ott, and G. Hirzinger, "A unified passivity-based control framework for position, torque and impedance control of flexible joint robots," *The International Journal of Robotics Research*, vol. 26, no. 1, pp. 23–39, January 2007.

[21] T. Wimböck, Ch. Ott, and G. Hirzinger, "Passivity-based object-level impedance control for a multifingered hand," in *IEEE/RSJ Int. Conference on Intelligent Robots and Systems*, 2006, pp. 4621–4627.

[22] Ch. Ott, O. Eiberger, W. Friedl, B. Bäuml, U. Hillenbrand, Ch. Borst, A. Albu-Schäffer, B. Brunner, H. Hirschmüller, S. Kielhöfer, R. Konietschke, M. Suppa, T. Wimböck, F. Zacharias, and G. Hirzinger, "A humanoid two-arm system for dexterous manipulation," in *IEEE-RAS International Conference on Humanoid Robots*, 2006, pp. 276–283.

[23] T. Wimböck, Ch. Ott, and G. Hirzinger, "Impedance behaviors for two-handed manipulation: Design and experiments," in *IEEE Int. Conf. on Robotics and Automation*, 2007, pp. 4182–4189.

[24] G. A. Pratt and M. M. Williamson, "Series elastic actuators," in *IEEE/RSJ Int. Conference on Intelligent Robots and Systems*, 1995, pp. 399–406.

[25] J. Pratt and G. Pratt, "Exploiting natural dynamics in the control of a planar bipedal walking robot," in *Proceedings of the Thirty-Sixth Annual Allerton Conference on Communication, Control, and Computing*, 1998.

[26] J. Pratt and B. Krupp, "Design of a bipedal walking robot," in *Proceedings of the 2008 SPIE*, vol. 6962, 2008.

[27] T. McGeer, "Passive dynamic walking," *The International Journal of Robotics Research*, vol. 9, no. 2, pp. 62–82, 1990.

[28] S. Collins, A. Ruina, R. Tedrake, and M. Wisse, "Efficient bipedal robots based on passive dynamic walkers," *Science*, vol. 307, no. 5712, pp. 1082–1085, 2005.

[29] A. D. Kuo, "Energetics of actively powered locomotion using the simples walking model," *Journal of Biomechanical Engineering*, vol. 124, pp. 113–120, 2002.

[30] F. Asano, M. Yamakita, N. Kamamichi, and Z.-W. Luo, "A novel gait generation for biped walking robots based on mechanical energy constraint," *IEEE Transactions on Robotics*, vol. 20, no. 3, pp. 565–573, 2004.

[31] G. Hirzinger, N. Sporer, A. Albu-Schäffer, M. Hähnle, R. Krenn, A. Pascucci, and M. Schedl, "DLR's torque-controlled light weight robot III - are we reaching the technological limits now?" in *IEEE Int. Conf. on Robotics and Automation*, 2002, pp. 1710–1716.

[32] F. Kanehiro, K. Fujiwara, S. Kajita, K. Yokoi, K. Kaneko, H. Hirukawa, Y. Nakamura, and K. Yamane, "Open architecture humanoid robotics platform," in *IEEE Int. Conf. on Robotics and Automation*, 2002, pp. 24–30.

[33] B. Bäuml and G. Hirzinger, "When hard realtime matters: Software for complex mechatronic systems," *Robotics and Autonomous Systems*, vol. 56, pp. 5–13, 2008.

[34] S. Kajita, F. Kanehiro, K. Kaneko, K. Fujiwara, K. Harada, K. Yokoi, and H. Hirukawa, "Biped walking pattern generation by using preview control of zero-moment point," in *Proceedings of the IEEE International Conference on Robotics and Automation*, 2003, pp. 1620–1626.

[35] Y. Choi, Y. Bum-Jae, and K. Doik, "On the walking control for humanoid robot based on the kinematic resolution of com jacobian with embedded motion," in *Proceedings of the IEEE International Conference on Robotics and Automation*, 2006, pp. 2655–2660.

[36] T. Sugihara, Y. Nakamura, and H. Inoue, "Realtime humanoid motion generation through zmp manipulation based on inverted pendulum control," in *Proceedings of the IEEE International Conference on Robotics and Automation*, 2002, pp. 1404–1409.

[37] S.-H. Hyon and G. Cheng, "Gravity compensation and full-body balancing for humanoid robots," in *Proceedings of the IEEE/RAS International Conference on Humanoid Robots*, 2006, pp. 214–221.

[38] D. Lee and Y. Nakamura, "Mimesis model from partial observations for a humanoid robot," *Int. Journal of Robotics Research*, vol. 29, no. 1, pp. 60–80, 2010.

[39] L. R. Rabiner, "A tutorial on hidden markov models and selected applications in speech recognition," *Proc. IEEE*, vol. 77(2), pp. 257–286, 1989.